Cell Reports, Volume *29*

Supplemental Information

IL-12 Blocks Tfh Cell Differentiation during *Salmonella* Infection, thereby Contributing to Germinal Center Suppression

Rebecca A. Elsner and Mark J. Shlomchik

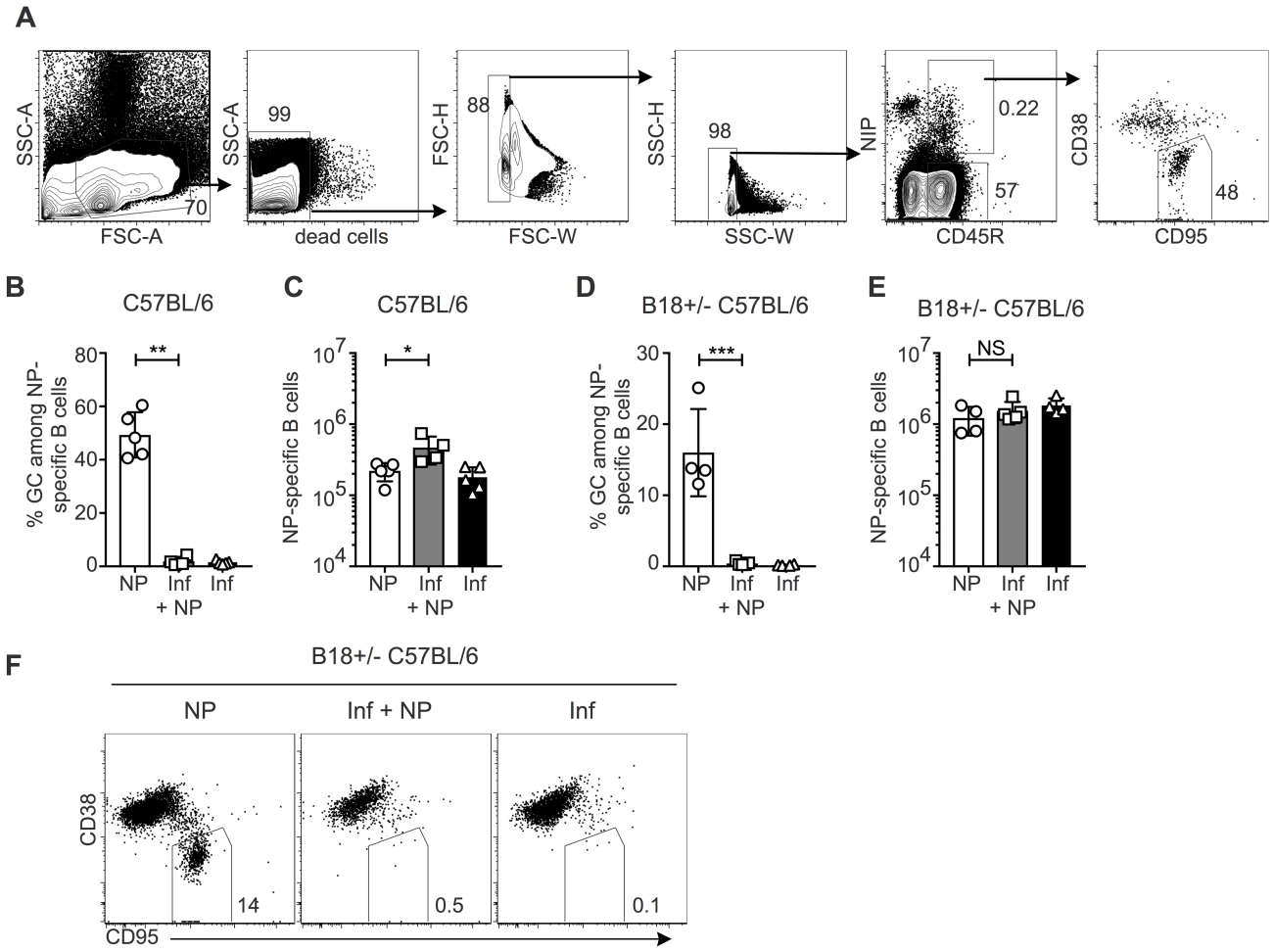

Supplemental Figure 1. STm infection suppresses splenic GC in both wild type and NP-specific BCR transgenic mice, Related to Figure 1. (A-D) Additional data from Figure 1. (A) Representative plots showing gating scheme for NIP-binding GC B cells. Contour plots are 5% with outliers, and the final plot of NIP-binding B cells is a dot plot showing all events. (B) Quantification of the number of NIP-binding B cells per spleen, and the frequencies of GC among them (C) in C57BL/6 mice. (D-F) Number of NIP-binding B cells per spleen (D), and the frequency of GC B cells among them (E) in B1-8+/- C57BL/6. (F) Representative dot plots of live, singlet, NIP-binding B cells with gates indicating GC B cells from B18+/- C57BL/6 mice. Data points indicate individual mice (n=4-5 per group), and bars the mean ± SD. One representative experiment of 2 is shown from C57BL/6 mice, and one experiment in B18+/- C57BL/6 mice. Statistical significance was calculated by one-tailed Student's t Test, NS = not significant, * $P<0.05$, ** $P<0.01$, *** $P<0.001$.

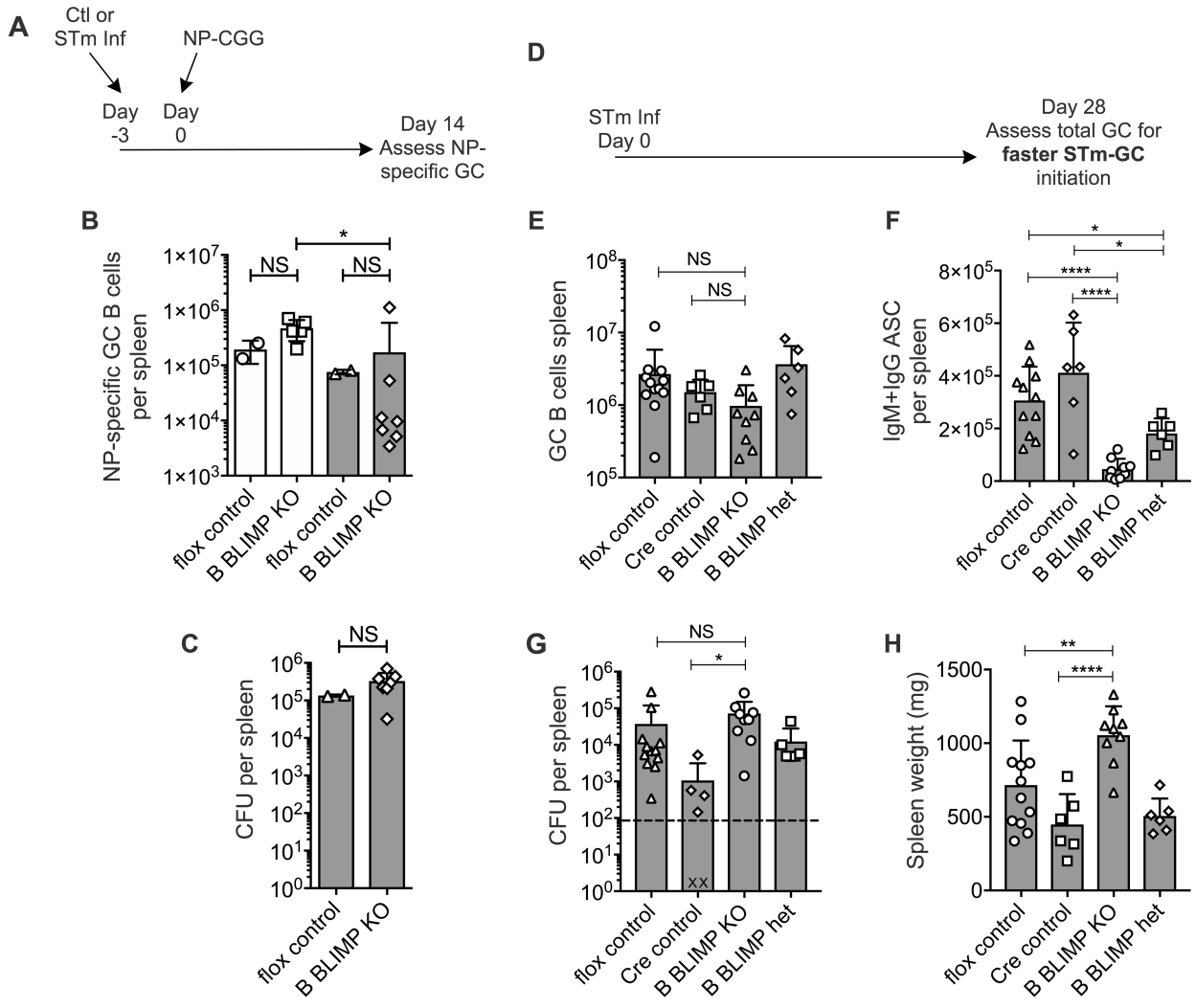

Supplemental Figure 2. Blocking plasma cell differentiation does not rescue GC responses, Related to Figure 3. (A-C) Experimental design (A): BLIMP-1$^{flox/flox}$ (flox control), and CD19-Cre^{+} BLIMP-1$^{flox/flox}$ (B BLIMP KO) mice were infected with STm on day -3, then immunized with NP-CGG in alum on day 0, and splenic NP-specific B cell responses were assessed 14 days post NP-immunization. (B) NP-specific GC B cells were quantified by flow cytometry from control (white bars) or STm infected mice (gray bars). (C) Bacterial CFU per spleen were not significantly different among infected groups. Data points indicate individual mice (n=2-6 per group), and bars the mean ± SD of one experiment. (D-H) Experimental design (D): BLIMP-1$^{flox/flox}$ (flox control), CD19-Cre^{+} (Cre control), CD19-Cre^{+} BLIMP-1$^{flox/flox}$ (B BLIMP KO), and CD19-Cre^{+} BLIMP-1$^{flox/wt}$ (B BLIMP het) spleens were analyzed 28 days after STm infection for early induction of GC B cells by FACS analysis (E), antibody secreting cells (ASC) by ELISPOT (F), bacterial burdens (G), and spleen organ weights (H). Data points indicate individual mice (n=5-8 per group), and bars the mean ± SD. Dashed lines (G) represent the limit of detection, and grey "X" indicate spleens with no CFU detected. Data are pooled from two independent experiments, n=3-9 per group per experiment for B BLIMP KO and flox control groups, and n=1-5 for Cre control and B BLIMP het groups. Statistical significance was calculated by two-tailed Student's t Test (B-C), and Mann-Whitney two-tailed test (E-H) to include an outlier with 1 log lower bacterial burden, NS = not significant, * P<0.05, ** P<0.01, *** P<0.001, **** P<0.0001.

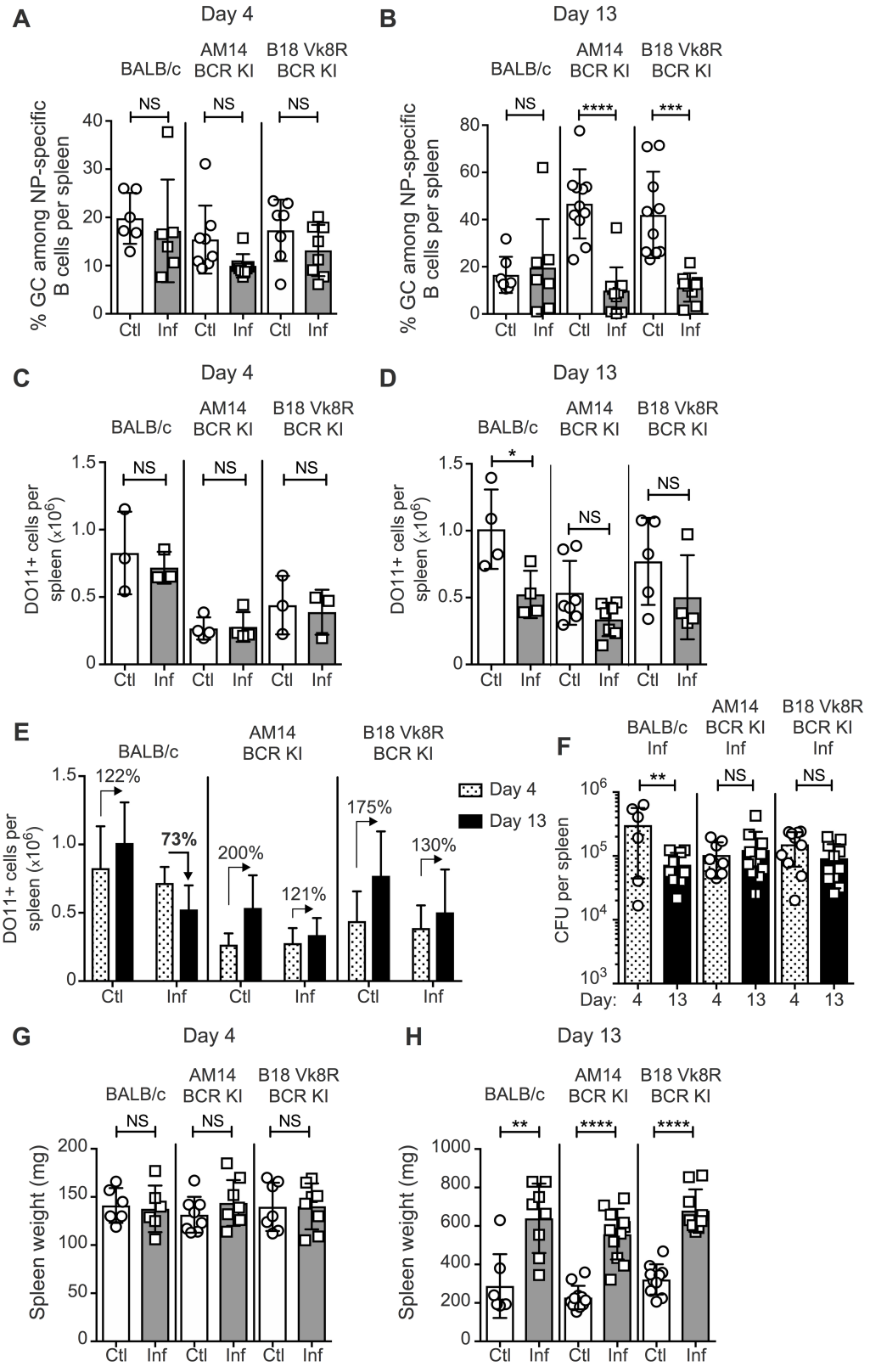

Supplemental Figure 3. STm infection suppresses NP-OVA induced GC despite equal numbers of OVA-specific T cells, Related to Figure 2. (A-E) Additional data from Figure 2. BALB/c or BCR-restricted AM14 BCR knock in (AM14 KI) BALB/c, or B18+/+ heavy VK8R+/- light chain knock in (B18 Vk8R KI) mice received NP-specific B and OVA-specific DO11.10+ CD4+ T cells on day -1, control (Ctl) or STm infection (Inf) on day 0 and NP-OVA in alum approximately 4 hours later. Splenic NP-specific B cells and DO11+ T cells were analyzed by flow cytometry on days 4 and 13 post infection/immunization. (A-B) Frequencies of GC cells among NP-specific B cells per spleen at 4 days (A) and 13 days post NP-OVA (B). (C-D) Number of live, singlet, CD19- CD4+ DO11+ T cells per spleen at days 4 (C) and 13 (D). (E) The percent change in the mean number of DO11+ cells per spleen between day 4 and 13 relative to day 4, for each group. (F) Bacterial burden of infected mice only at days 4 and 13 post

infection/immunization. Spleen weights at days 4 (G) and 13 (H), note differences in Y-axis scale. Data points indicate individual mice (n=3-5 per groups), and bars the mean ± SD of 3 experiments pooled (A-D, F-H) or one experiment (E). Statistical significance was calculated by one-tailed Student's t Test, NS = not significant, * $P<0.05$, ** $P<0.01$, *** $P<0.001$, **** $P<0.0001$.

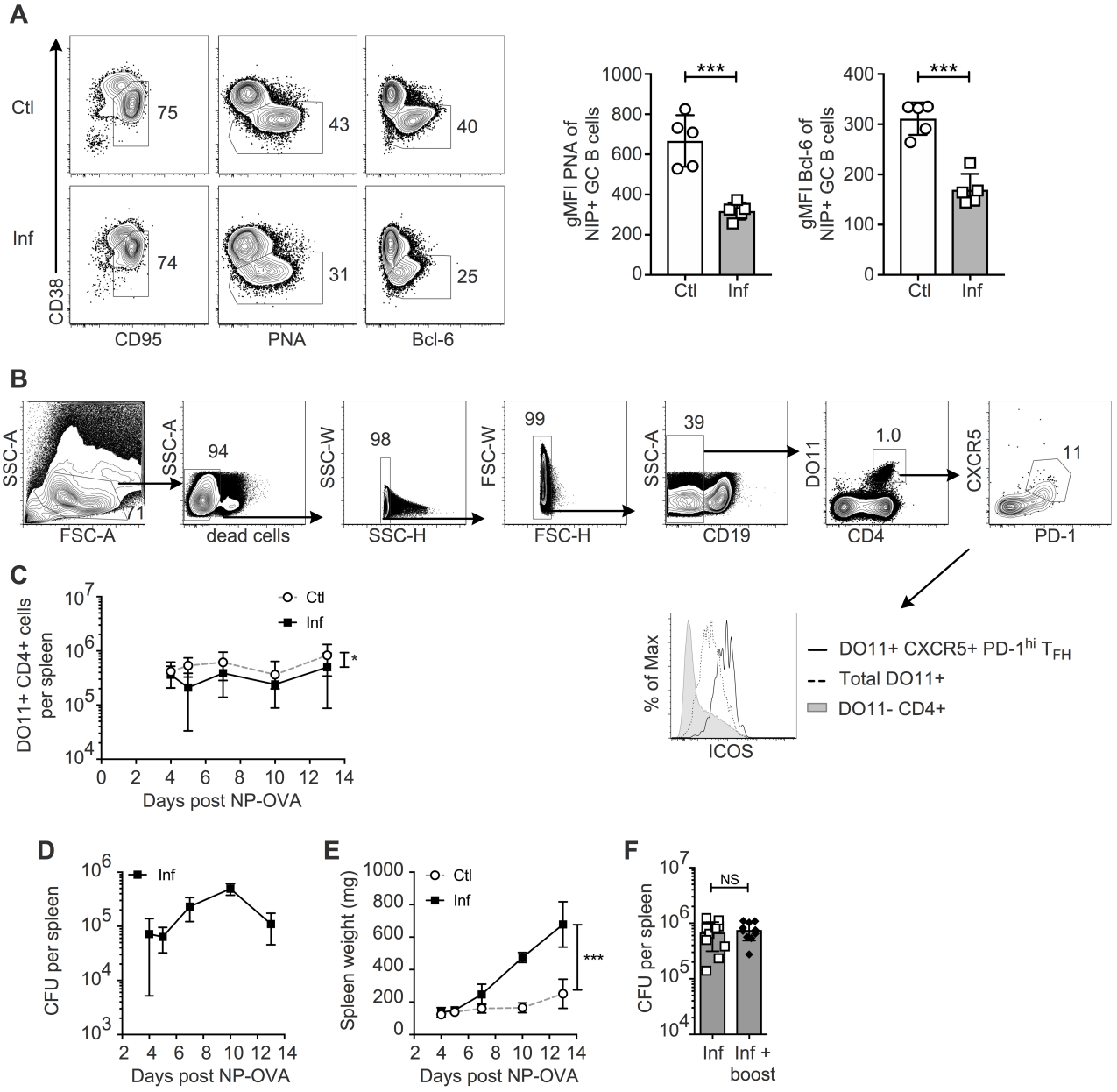

Supplemental Figure 4. Expansion of transferred DO11 cells is somewhat reduced in STm infected mice, Related to Figure 4. (A-E) BALB/c B18+/+ heavy VK8R+/- light chain knock in (B18 Vk8R KI) host mice were treated as described in Figure 3A and splenic NIP-binding B cells and DO11+ T_{FH} were quantified by FACS on days 4-13 post infection/immunization. (A) Representative FACS plots and graphs from day 7 comparing phenotypic markers of GC B cells, gated on live, singlet, NIP-binding CD19+ B cells. The CD38 vs CD95 gate was used through the time course to quantify GC B cells. PNA and Bcl-6 staining were performed in one experiment on day 7 while CD38 vs CD95 was performed throughout the time course. Charts show geometric mean fluorescent intensity (gMFI) of PNA and Bcl-6 on NP-specific GC B cells. (B) Shown are representative FACS plots used to identify DO11+ T_{FH} from one mouse of the control group and a histogram comparing DO11+ T_{FH} to other T cell populations for ICOS expression. (C) Numbers of DO11+ T cells were quantified at indicated times post NP-OVA immunization. Bacterial CFU per spleen (D) and spleen weights (E) over time. (F) Bacterial CFU of infected mice without, and with, NP-CGG boost from Fig. 4. Data are pooled from three independent experiments with 3-5 mice per group per time point. All FACS plots are 5% contour plots with outliers. Data points indicate the mean and error bars ± SD. Statistical significance was calculated by Student's t test *** P<0.001 (A) and two-way ANOVA, * P<0.05 (C).

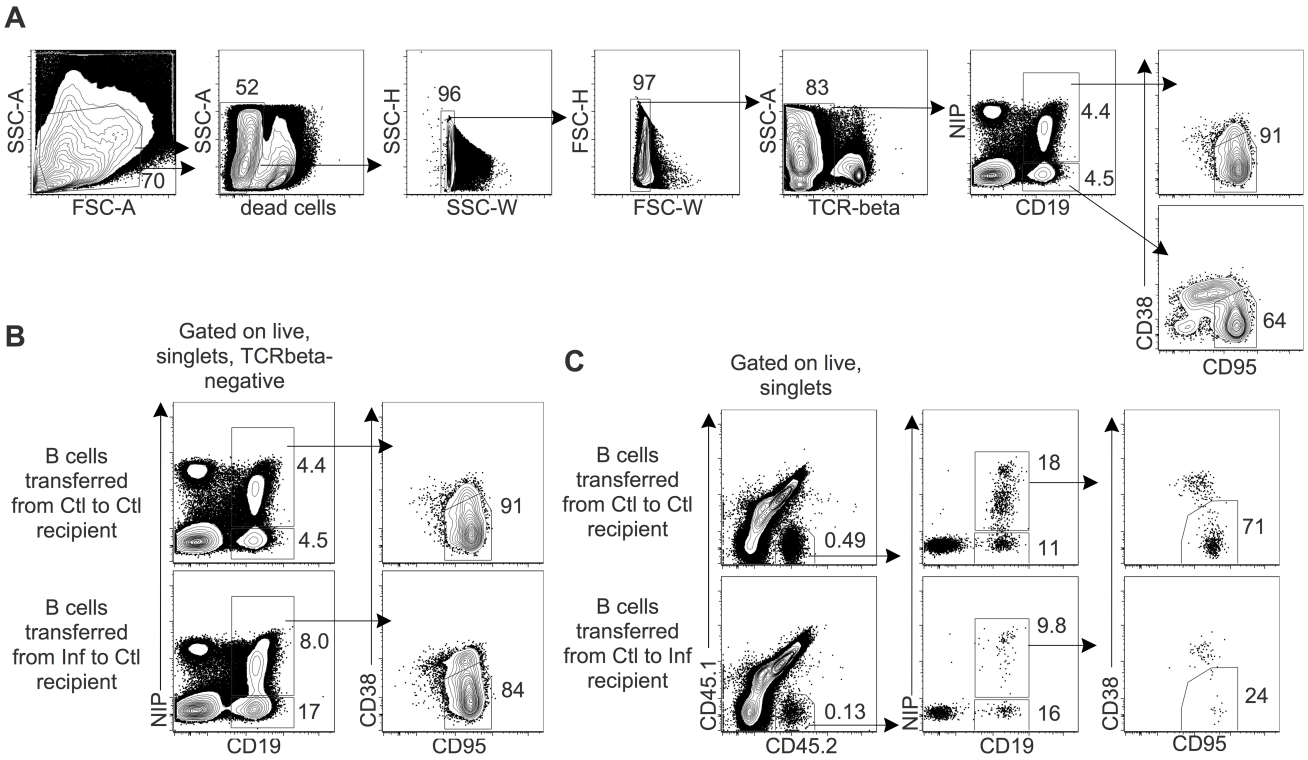

Supplemental Figure 5 Example flow cytometry gating, Related to Figure 5. (A-B) Example of the gating used to identify NP-specific germinal center B cells after transfer from Ctl or Inf primary hosts into Ctl secondary hosts as described in Figure 6A. Ctl to Ctl example from B was the same sample as was used in A. (C) Example of the gating used to identify CD45.2 cells after being primed in Ctl hosts and transferred into Ctl or Inf secondary hosts. Events shown were previously gated on live singlet TCR-beta-negative as in A. All plots are 5% contour with outliers except the 2 center and 2 right plots in (C) which are dot plots.

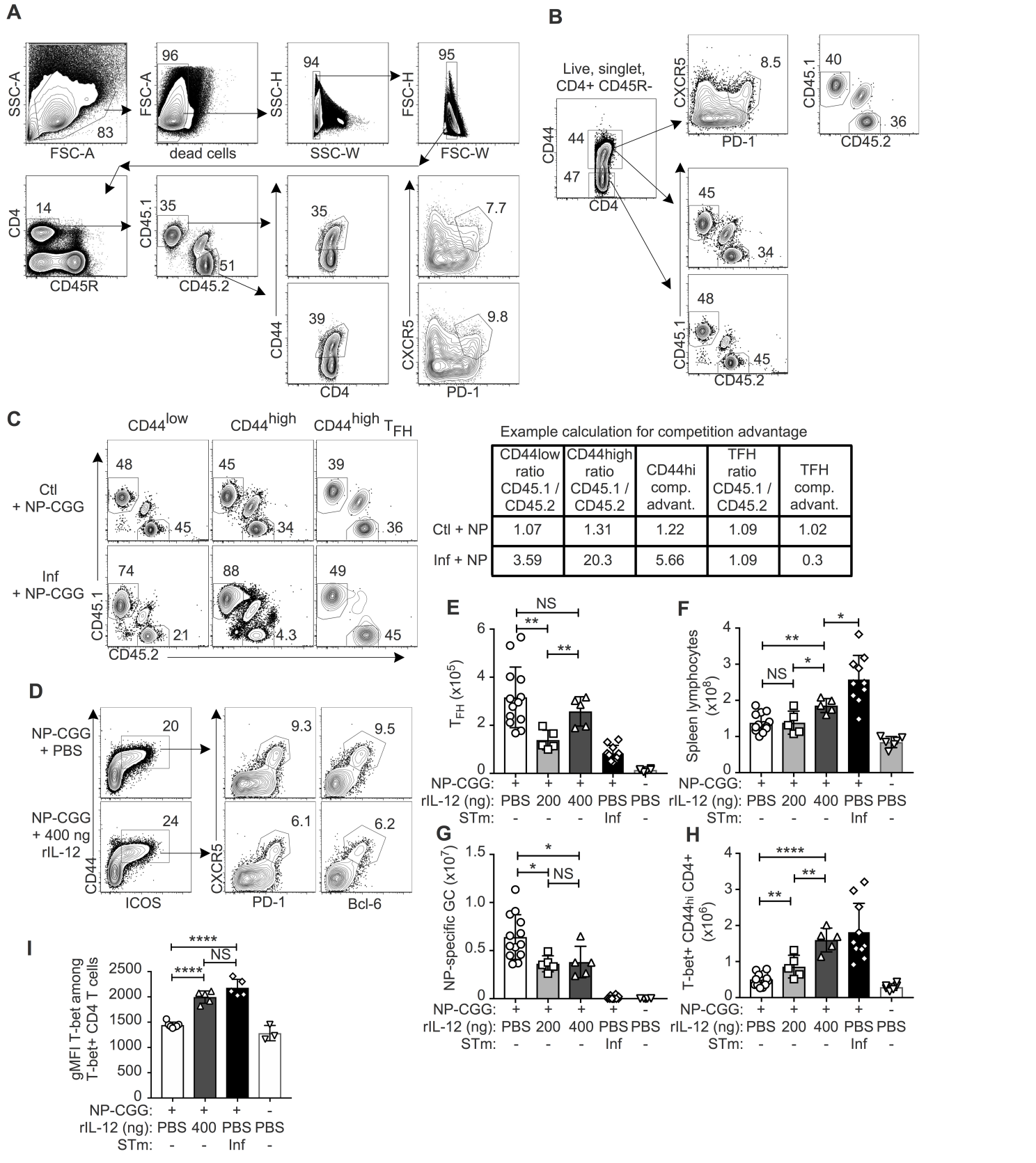

Supplemental Figure 6 IL-12 suppresses T_{FH} differentiation, Related to Figure 6. (A) Example of gating used to identify CXCR5+ PD-1^{high} T_{FH} among $CD44^{high}$ T cells of either CD45.1 or CD45.2 KO origin for Figure 7 A-G. (B) Example of how the ratio of WT/KO cells were quantified among $CD44^{low}$, $CD44^{high}$, and T_{FH} populations from either control or STm infected mice (C) and used to calculate the fold competitive advantage of one representative sample from each group, where competitive advantage is equal to the CD45.1/CD45.2 ratio for $CD44^{high}$ or T_{FH} divided by the base ratio of $CD44^{low}$ naïve T

cells to normalize for differences in engraftment of each bone marrow between mice. (D-I) NP-CGG immunized mice were treated 4x with 400 ng recombinant IL-12 (rIL-12) or PBS control. (D) Representative examples of T_{FH} gating from $CD44^{high}$ ICOS+ cells are plotted twice switching the x-axis to show CXCR5 expression in comparison to PD-1 or Bcl-6, all CXCR5+ cells were both $PD\text{-}1^{high}$ and Bcl-6+. Numbers of T_{FH} (E), NP-specific GC (F), and T-bet+ CD4+ T cells (G) were quantified by flow cytometry at day 9 post treatment with rIL-12 as described in Figure 7G, and the total number of splenic lymphocytes per mouse by trypan blue count (H). (I) Geometric mean fluorescent intensity (gMFI) of intracellular T-bet staining on T-bet+ CD4 T cells. This analysis was only performed on the 400 ng treatment experiment. All FACS plots for A-D are 5% contour with outliers. For all charts, symbols represent individual mice (n=3-7 per group) and bars the mean ± SD. Statistical significance was calculated by two-tailed Student's t test, NS = not significant, * $P<0.05$, ** $P<0.01$, *** $P<0.001$, **** $P<0.0001$.

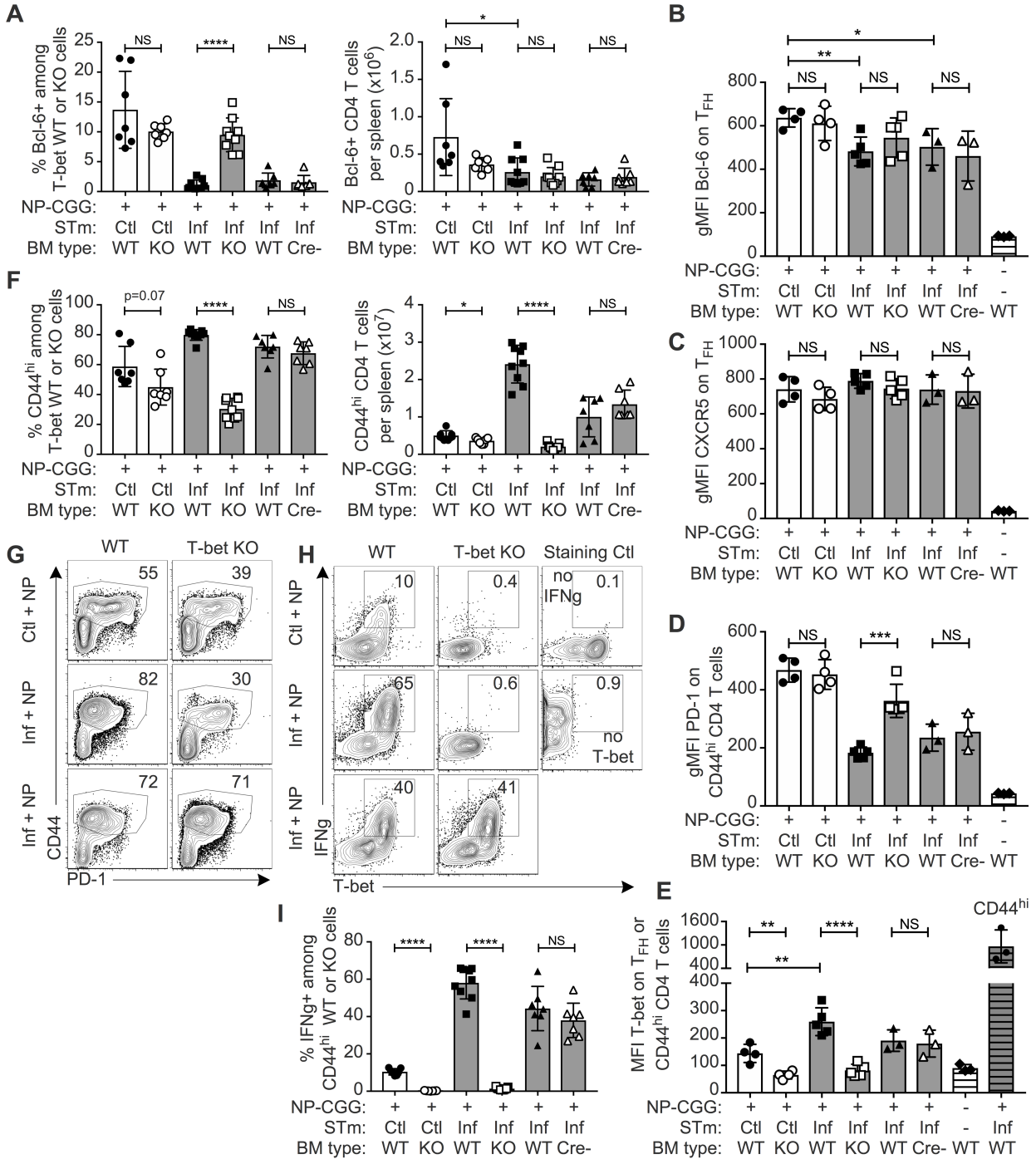

Supplemental Figure 7 T-bet suppresses T_{FH} differentiation but promotes expansion, Related to Figure 7. (A) Percent and number of T cells expressing Bcl-6 by intracellular staining from either T-bet WT or KO cells in mixed bone marrow chimeras described in Fig. 7. Geometric mean fluorescent intensity (gMFI) of Bcl-6 (B), CXCR5 (C), PD-1 (D), and T-bet (E) on T_{FH} from either T-bet WT or KO cells from one experiment of two. White striped bars show $CD44^{low}$ T cells from naïve chimeras, and gray striped bars WT $CD44^{high}$ T cells from infected chimeras for relative comparison. (F) Percent and number of activated $CD44^{high}$ CD4 T cells from either T-bet WT or KO cells. Representative FACS plots of the percent of $CD44^{high}$ cells (G), and the percent of IFNg-producing cells among $CD44^{high}$ T cells (H) in T-bet WT or KO cells from each treatment group. (I) Percent IFNg-producing cells from each cell/treatment type. All FACS plots for are 5% contour with outliers. For all charts, symbols represent individual mice (n=3-7 per group), and bars the mean ± SD. For charts C-F, one experiment of 2 is shown, for all other charts data were combined from 2 experiments. Statistical significance was calculated by two-tailed Student's t test, NS = not significant, * P<0.05, ** P<0.01, *** P<0.001, **** P<0.0001.